Historical Biology, 2014
Vol. 26, No. 1, 110–121, http://dx.doi.org/10.1080/08912963.2012.763119

Taylor & Francis
Taylor & Francis Group

Osteohistological insight into the early stages of growth in *Mussaurus patagonicus* (Dinosauria, Sauropodomorpha)

Ignacio Alejandro Cerda[a,b]*, Diego Pol[a,c] and Anusuya Chinsamy[d]

[a]*Consejo Nacional de Investigaciones Científicas y Técnicas (CONICET), Universidad Nacional de Río Negro, Museo Carlos Ameghino, Belgrano 1700, Paraje Pichi Ruca (predio Marabunta), 8300 Cipolletti, Río Negro, Argentina;* [b]*Instituto de Investigación en Paleobiología y Geología, Universidad Nacional de Río Negro, Museo Carlos Ameghino, Belgrano 1700, Paraje Pichi Ruca (predio Marabunta), 8300 Cipolletti, Río Negro, Argentina;* [c]*Museo Paleontológico Egidio Feruglio, Avenida Fontana 140, Trelew, 9100 Chubut, Argentina;* [d]*Biological Sciences Department, University of Cape Town, Private Bag, Rondebosch, 7700 Cape Town, South Africa*

(*Received 23 November 2012; final version received 29 December 2012; first published online 4 February 2013*)

Here, we describe the bone histology of juvenile specimens of the basal sauropodomorph *Mussaurus patagonicus* and interpret its significance in terms of the early growth dynamics of this taxon. Thin sections from three juvenile specimens (femur length, 111–120 mm) of *Mussaurus* were analysed. The sampled bones consist of multiple postcranial elements collected from the Late Triassic Laguna Colorada Formation (El Tranquilo Group, Patagonia). The cortical bone is composed of fibrolamellar bone tissue. Vascularisation is commonly laminar or plexiform in the long bones. Growth marks are absent in all the examined samples. The 'epiphyses' of long bones are all formed by well-developed hypertrophied calcified cartilage. The predominance of woven-fibred bone matrix in cortical bones indicates a fast growth rate in the individuals examined. Moreover, given the existence of growth marks in adult specimens of *Mussaurus*, as in other sauropodomorphs, and assuming that the first lines of arrested growth was formed during the first year of life, the absence of growth marks in all the bones suggest that the specimens died before reaching their first year of life. Compared with the African taxon *Massospondylus carinatus* (another basal sauropodomorph for which the bone histology has been previously studied), it appears that *Mussaurus* had a higher early growth rate than *Massospondylus*.

Keywords: histology; growth rates; Dinosauria; basal Sauropodomorpha

1. Introduction

Mussaurus patagonicus was first described on the basis of eight associated post-hatchling individuals from Upper Triassic beds of southern Argentina (Bonaparte and Vince 1979). Closely associated with these young individuals, two complete eggs and eggshell fragments were found. These specimens were collected from the Laguna Colorada locality (Santa Cruz Province, Argentina), in sediments of the Laguna Colorada Formation (El Tranquilo Group; Herbst 1965; Jalfin and Herbst 1995). Bonaparte and Vince (1979) suggested 'prosauropod' affinities of *M. patagonicus* but the extremely early ontogenetic stage of these individuals precluded the establishment of more precise affinities. Recently, Pol and Powell (2007) assigned to *M. patagonicus* additional material from the same unit and locality. These remains consist of partially articulated remains of at least 14 juvenile specimens (Figure 1), which are approximately four times larger than the post-hatchling specimens (post-hatchling femur length, 30 mm; largest juvenile femur length, 120 mm). The record of the first stages of development in *M. patagonicus* allows several paleobiological assessments, including the changes in the bone histology during the early stages of the development.

Bone microstructure (histology) is well recognised as providing information about the biology of extinct vertebrates, and has been extensively used in dinosaurs (e.g. Ricqlès 1980; Chinsamy-Turan 2005). It gives a direct record of ontogenetic growth and it provides clues concerning various aspects of dinosaur biology, including longevity (Chinsamy 1990, 1993; Varricchio 1993; Curry 1999), growth rates (Ricqlès 1980; Chinsamy 1993; Varricchio 1997; Erickson et al. 2001; Padian et al. 2004; Lehman and Woodward 2008; Werning 2012), age at maturity (Varricchio 1993; Sander 2000; Klein and Sander 2007; Lee and Werning 2008), adult size (Sander et al. 2006; Klein and Sander 2007; Stein et al. 2010; Company 2011), and ontogenetic stages and timing of sexual maturity (Sander 2000; Erickson et al. 2007; Lee and Werning 2008; Klein and Sander 2008; Hayashi et al. 2009; Hübner 2012). Although the number of paleohistological studies based on sauropodomorph dinosaurs is relatively abundant compared with other fossil taxa, these contributions are mainly focused on neosauropod taxa (Rimblot-Baly et al. 1995; Curry 1999; Sander 2000; Sander and Tückmantel 2003; Sander et al. 2006; Klein and Sander 2008; Woodward and Lehman 2009; Stein et al. 2010; Company 2011; Klein et al. 2012). In contrast, our knowledge about the histological and

*Corresponding author. Email: nachocerda6@yahoo.com.ar

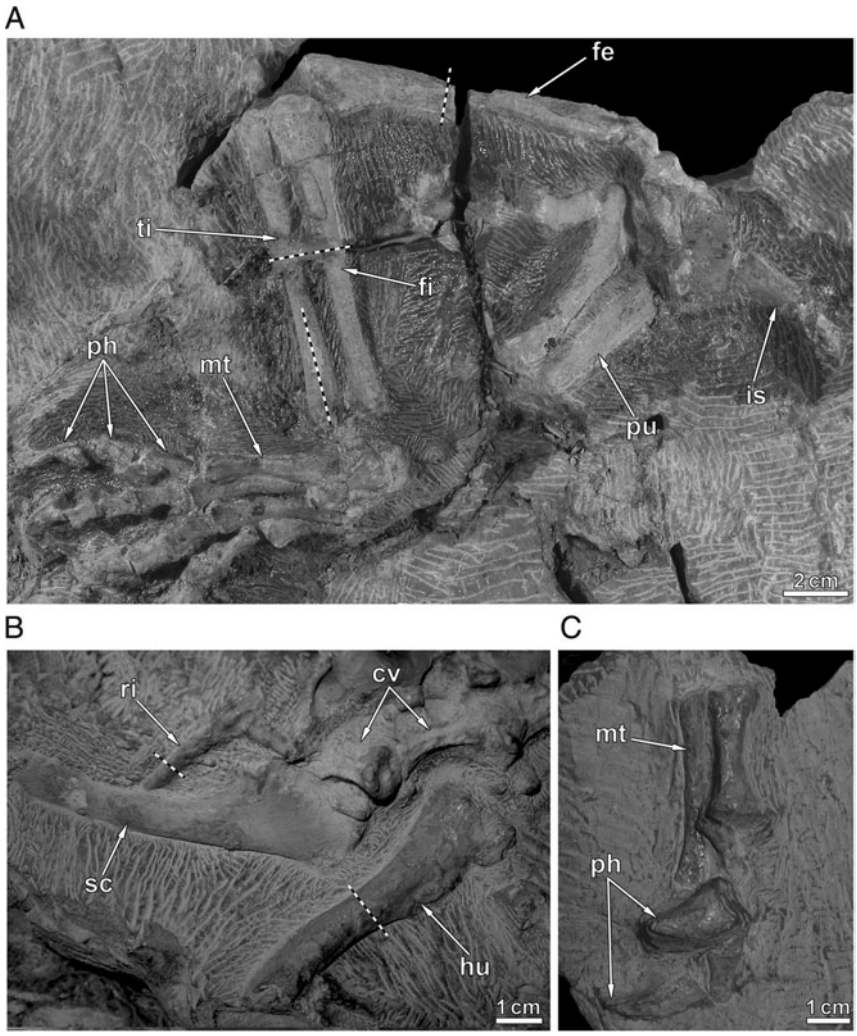

Figure 1. Postcranial bones of *M. patagonicus.* (A) Hind limb and pelvic girdle of specimen MPM-PV 1813/10. (B) Forelimb and scapular girdle of specimen MPM-PV 1813/13. (C) Pes of specimen MPM-PV 1813/2. Dashed lines indicate the approximate position of the thin sections of the principal bones sectioned in this study. Abbreviations: cv, cervical vertebrae; fe, femur; fi, fibula; hu, humerus; is, ischium; ph, phalanges; pu, pubis; mt, metatarsals; sc, scapula; ri, ribs; ti, tibia.

ontogenetic changes of basal sauropodomorphs is rather limited. To date, the most important studies on basal sauropodomorph histology has been focused on *Plateosaurus engelhardti* from the Late Triassic of Central Europe (Sander and Klein 2005; Klein and Sander 2007) and *Massospondylus carinatus* from the Early Jurassic of South Africa (Chinsamy 1993). The study of *Plateosaurus* was based on a large sample of long bones of different-sized specimens (femur length varies between 500 and 990 mm). One of the most important results from the latter study was the determination of a high variability of adult body size within this species, explained as an effect of environmental variations and phenotypic plasticity. Unfortunately, the available sample of specimens of *Plateosaurus* does not include specimen of early ontogenetic stages (Sander and Klein 2005; Klein and Sander 2007). In the case of *Massospondylus*, although the sample included a smaller number of specimens than in the study of *Plateosaurus*, a more complete ontogenetic series was analysed (femoral length size ranged between 120 and 440 mm) (Chinsamy 1993; Chinsamy-Turan 2005). The presence of growth rings in the cortical bone and the absence of a true outer circumferential layer in the cortical bone of *Massospondylus* were interpreted as indicators of a cyclical and indeterminate growth strategy in this taxon (Chinsamy 1993).

The main objective of this study is to characterise the bone histology of juvenile specimens of *M. patagonicus*, and to assess the early growth dynamics of this basal sauropodomorph. In addition, we compare the bone histology and growth rate of *M. patagonicus* with the results obtained for *M. carinatus*.

2. Institutional abbreviations

BP, Bernard Price Institute for Paleontological Research, University of the Witwatersrand, Johannesburg, South Africa; MPM-PV, Vertebrate Paleontology collection of the Museo Regional Provincial 'Padre Molina', Río Gallegos, Santa Cruz Province, Argentina; PVL, Vertebrate Paleontology collection of the Instituto Miguel Lillo, San Miguel de Tucumán, Tucumán Province, Argentina.

3. Materials and methods

Postcranial bones of three juvenile individuals of *M. patagonicus* (MPM-PV 1813/10, 1813/12 and 1813/8) were used in this study. The transverse thin sections from the specimen MPM-PV 1813/10 were generated from the mid-shaft of the femur, at the level of the fourth trochanter and below. To ensure no loss of gross morphologic data, the element was moulded prior to thin sectioning, and resin casts were made. In the case of the specimen MPM-PV 1813/12, thin sections consist of several unprepared bones located at the edge of the block that contained all specimens. The slices from this individual include transversal, longitudinal and oblique sections of several bones (humerus, femur, tibia, astragalus, ribs and undetermined elements). The sample obtained from MPM-PV 1813/8 consists of three dorsal ribs.

Specimens were prepared for thin sections based on the methodology outlined in Chinsamy and Raath (1992). The preparation of the histological sections was carried out in Egidio Feruglio Museum of Trelew (Argentina). All slices were studied using a petrographic polarising microscope. Nomenclature and definitions of structures used in this study are derived from Francillont-Vieillot et al. (1990) and Chinsamy-Turan (2005). Although not strictly accurate, we consider the channels within the bone to reflect the extent and organisation of vascularisation (Starck and Chinsamy 2002). The epiphyses in *Mussaurus*, as in all fossil juvenile animals, differ from those of living animals because although they are cartilaginous, the terminal surfaces are not true articular surfaces. Rather, they represent the interface between the lost uncalcified cartilage and the underlying calcified cartilage (Haines 1942; Reid 1997; Horner et al. 2000). Hence the 'true' epiphysis is almost entirely lost in fossil vertebrates, and our use of the term 'epiphyses' for fossil animals reflects this.

4. Results

4.1 General histological features

The long bones have an outer compact cortex surrounding a large medullary region. At the mid-shaft of long bones, there is a free marrow cavity that lacks an inner circumferential layer (ICL) of lamellar bone tissue. Cancellous bone commonly occupies the medullary region towards the proximal and distal ends of long bones. In the astragalus and autopodial bones, the cancellous bone generally completely infills medullary cavity. Bony trabeculae of cancellous bone consist of endosteal lamellar bone tissue. The cortical bone is composed of uninterrupted woven-fibred and fibrolamellar bone tissues. Vascular spaces are open or surrounded by a thin coat of lamellar bone tissue, indicating the early formation of primary osteons. Sub-periosteal vascular spaces commonly open to the outer surface. Although the organisation of the vascular spaces varies in different regions of the cortex (even in the same thin section), the laminar and plexiform are the most common patterns. Growth marks are absent in all the examined samples. Also, secondary osteons were not present. Although in fossil bones the outermost region of uncalcified cartilage is not preserved (Reid 1997; Chinsamy-Turan 2005), in long bones of *Mussaurus* the 'epiphyses' (Haines 1942) consist of a well-developed coating of hypertrophied calcified cartilage. This cartilage is commonly perforated by longitudinally oriented canals (transphyseal canals [Haines 1942; Reid 1997; Horner et al. 2000]). Apart from these general features, distinctive histological characteristics were observed in the different skeletal elements (details of which are presented below).

4.2 Humerus

In mid-shaft cross-sections, a highly vascularised bony cortex (2.1–3.3 mm of cortical thickness) encircles a well-developed, vacant marrow cavity. The cortex is entirely formed by fibrolamellar bone tissue consisting of a woven-fibred matrix with large open channels or only weakly developed primary osteons (Figure 2(A)). The woven-fibred matrix is isotropic under crossed polarised light and contains abundant globular osteocyte lacunae randomly distributed (Figure 2(B)–(D)). When present, primary osteons are composed of a few layers of lamellar bone with flattened osteocyte lacunae. Canaliculi from the osteocyte lacunae were not preserved. The pattern of vascularisation varies between a laminar and plexiform arrangement. Radial canals predominate in some areas. Several vascular spaces are opened to the sub-periosteal margins, which are considered as evidence of actively forming new bone at the periphery. A large channel (0.5 mm diameter) is observed penetrating the element from the outer surface. The medullary cavity margin of the cortex appears resorptive and lacks an ICL, suggesting that medullary expansion was still underway at the time of death. The innermost laminae of the cortex are partially resorbed. Growth marks (annuli or lines of arrested growth, LAGs) are absent in the cortical bone of this element.

4.3 Femur

The cortical bone at the mid-shaft region is composed of a well-vascularised cortex of primary fibrolamellar bone tissue. A large number of open channels traverse the cortical bone tissue, and in some places lamellar bone deposits occur centripetally to form early stages of primary osteons.

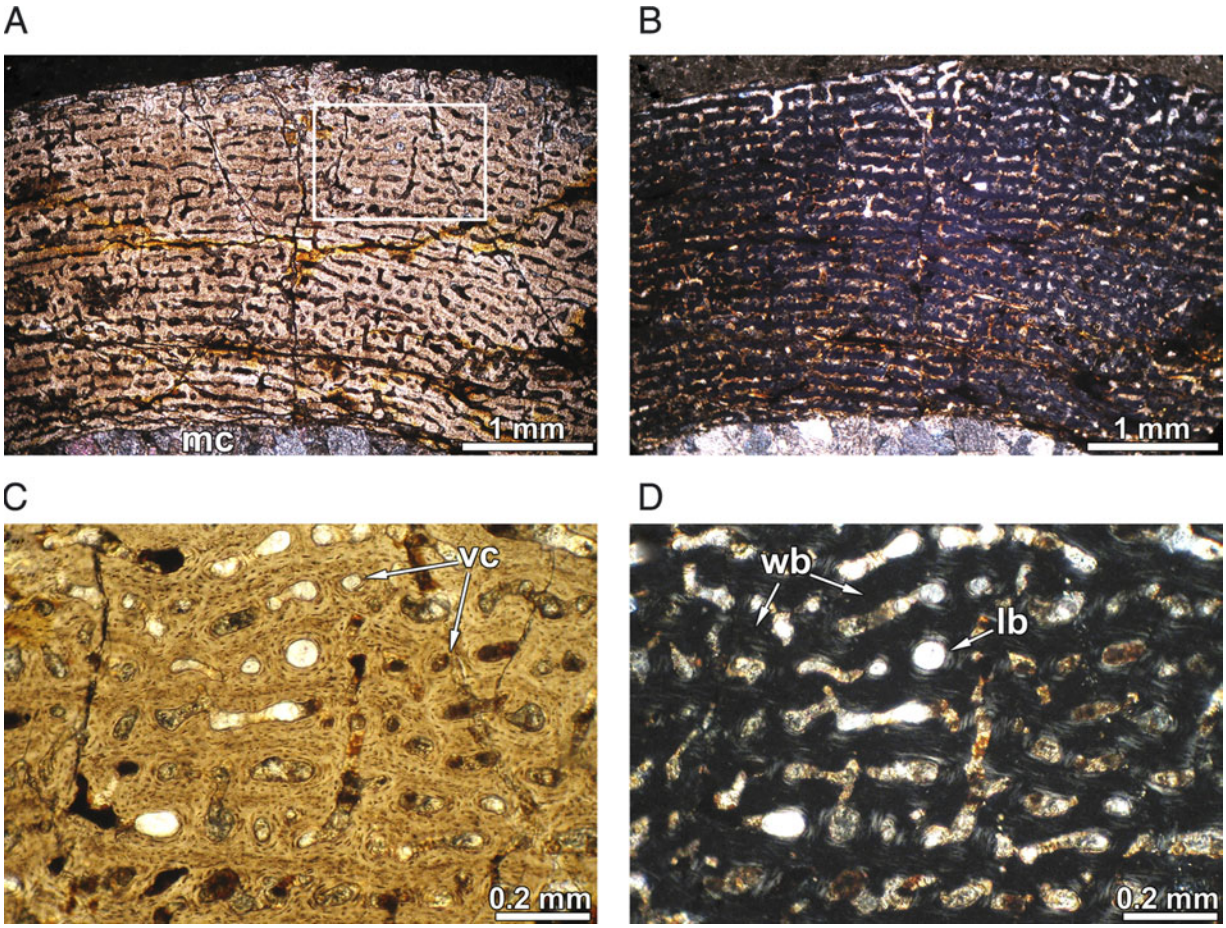

Figure 2. Histology of *M. patagonicus* humerus. (A) General view of the cortical bone showing abundant vascular canals. Normal light. (B) The same section under polarised light. (C) Enlarged view of the cortical bone (box inset in A). Primary osteons are in early stages of development, with only few layers of lamellar bone tissue around vascular canals. Normal light. (D) The same section under polarised light. Note the differences in the optical properties of the lamellar (birefringent) and woven-fibred (monorefringent) bone tissues. Abbreviations: lb, lamellar bone tissue; mc, medullary cavity; vc, vascular canals; wb, woven-fibred bone tissue.

Vascular networks display a laminar to plexiform pattern, with predominance of radial anastomoses in some areas (e.g. anterior cortex) making it more reticular in arrangement (Figure 3(A),(B)). Around the medullary cavity several laminae are partially resorbed and vascular spaces open directly to the perimedullary margin, suggesting that the medullary cavity is enlarging by erosion of the innermost (hence, earliest) periosteally formed bone. A large (average 0.78 × 0.54 mm) nutrient canal is visible in the lateroposterior region of the cortex (Figure 3(C)). The cortical bone tissue in the area of the fourth trochanter strongly differs from the other regions of the compacta (Figure 3(D)). In this area, the inner cortex contains several resorption cavities of irregular shape that results in a fine cancellous bone tissue (Figure 3(E)). This fine cancellous bone occupies the core area of the fourth trochanter and reaches the outer cortex. The innermost located bony trabeculale are composed of layers of endosteal lamellar tissue deposited during successive generations. The cortex of the distal edge of the fourth trochanter contains vascular spaces radially oriented and coated by a thin layer of lamellar bone. The bone matrix is composed of coarse Sharpey's fibre bundles (approximately 8 μm diameter of the transversally cut fibres) (Figure 3(F)). The main histological characters of the fourth trochanter observed in *Mussaurus* (predominance of radial canals extending in the direction of growth of the trochanter, presence of coarse Sharpey's fibres) has been reported in other dinosaurs (Horner et al. 2000, 2001, 2009; Cerda and Chinsamy 2012), and is a clear reflection of the influence of the *caudofemoralis longus* muscle in the development of the femur.

In one of the blocks that contains several limb bone sections of the specimen MPM-PV 1813/12, we identify and describe a transversal section of the distal portion of the femur. Except for the region that corresponds with the intercondylar sulcus, the bone in this sample is composed almost entirely of cancellous bone tissue (Figure 3(G)). The bony trabeculae are thin (30–80 μm) and they are

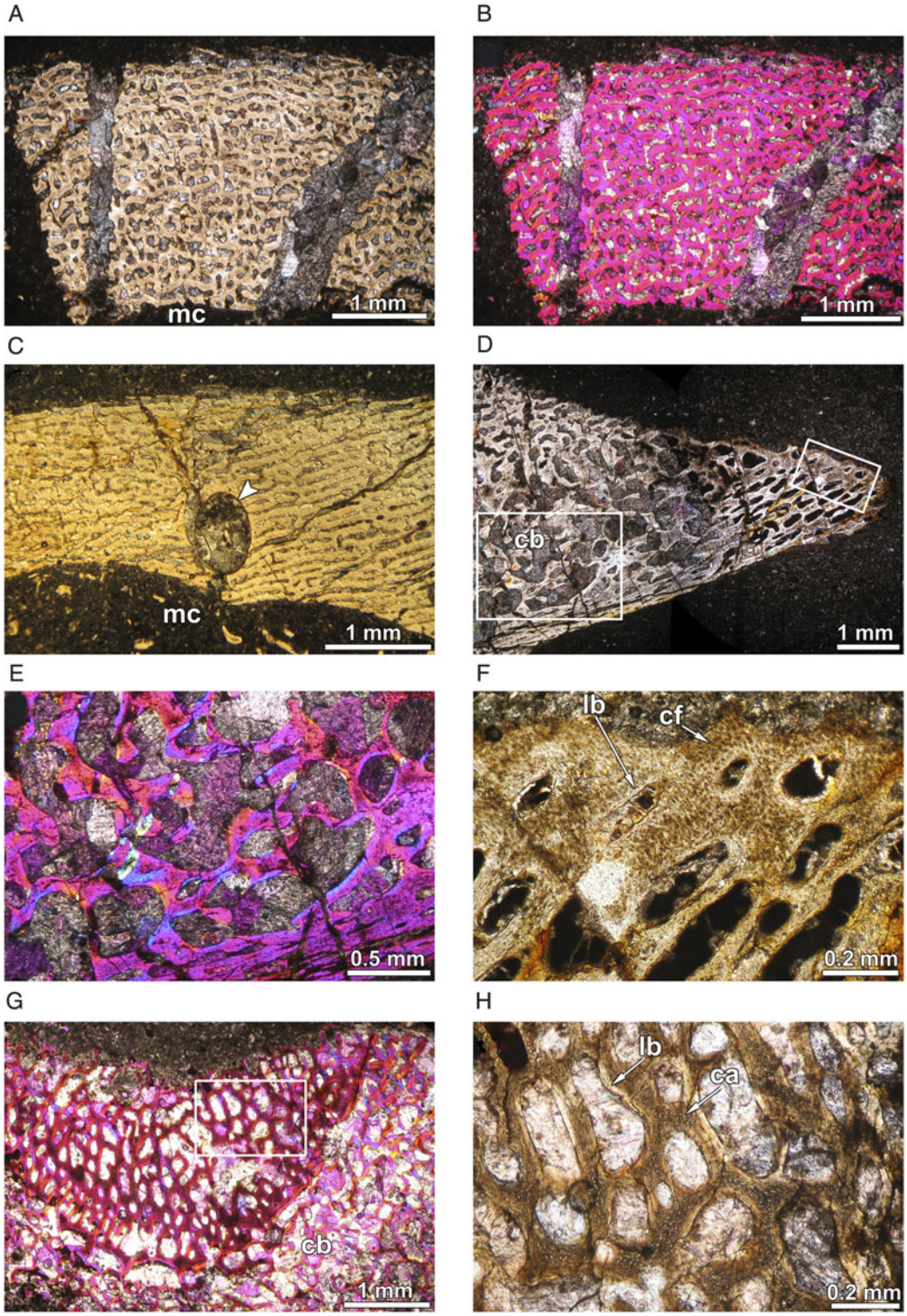

Figure 3. Histology of *M. patagonicus* femora. (A) Cortical bone in cross section. The cortex is formed by a well-vascularised woven-fibred bone matrix. Normal light. (B) The same section viewed under polarised light with lambda compensator. (C) General view of the cortex showing a prominent vascular space (arrowhead). Normal light. (D) Cross section of the fourth trochanter. Note the irregular shape of the resorption cavities in the cancellous bone. Normal light. (E) Details of the cancellous bone in the inner region of the fourth trochanter (larger box inset in D). Polarised light with lambda compensator. (F) Enlarged view of the distal portion of the fourth trochanter (smaller box inset in D). The bone matrix is composed of coarse fibre bundles. Normal light. (G) Cross section at the distal end region. While the internal bone consists of cancellous bone tissue, the cortex is formed by calcified cartilage. Polarised light with lambda compensator. (H) Detailed view (box inset in G) of the calcified cartilage. Normal light. Abbreviations: ca, calcified cartilage; cb, cancellous bone; cf, coarse fibre bundles; lb, lamellar bone tissue; mc, medullary cavity.

formed by lamellar bone tissue. The cortical bone between the tibial and fibular condyles consists of hypertrophied calcified cartilage. Chondrocyte lacunae are rounded in shape and they have diameters of roughly 0.01 mm (Figure 3(H)). The calcified cartilage contains several vascular spaces lined by a thin coat of lamellar bone.

4.4 Tibia

We examine transverse and longitudinal sections of two tibiae from the same individual. As described for other long bones, the transverse section of the tibia reveals an outer compact cortex surrounding a large medullary region. The cortical bone consists of uninterrupted fibrolamellar bone tissue, with a laminar and reticular organisation of the vascularisation. Several resorption cavities are observable in some regions of the perimedullary cortex.

The longitudinal section of the tibia includes the distal shaft and the distal 'epiphysis' of the element. The distal shaft is composed of a thin cortex of compact bone that encircles a vacant medullary cavity. The thickness of the compact bone (3.1 mm in the thicker region preserved) in this region decreases towards the epiphyseal end. Laminar vascularisation predominates in this region. Cancellous bone tissue is evident in the medullary cavity about 36 mm away from the distal end and progressively increases in thickness distally. Bony trabeculae consist of remains of non-resorbed periosteal bone and endosteal lamellar bone tissue. The distal end of the tibia consists internally of cancellous bone tissue. The 'articular' surface consists of hypertrophied calcified cartilage (Figure 4(A)). This cartilage is composed of chondrocyte lacunae that are irregularly arranged, as described for other non-avian dinosaurs (e.g. *Dryosaurus* [Chinsamy, 1995]; *Dysalotosaurus* [Hübner, 2012]; *Gasparinisaura* [Cerda and Chinsamy, 2012]) (Figure 4(B)). The chondrocyte lacunae are rounded and they have diameters of roughly 0.02 mm. The hypertrophied calcified cartilage is perforated by numerous longitudinally oriented tubules (transphyseal canals). Their walls are lined by a thin (approximately 30 μm) layer of lamellar bone. Towards the diaphysis, widening and fusion of the internal tubules leads to a cancellous bone tissue where remnants of calcified cartilage are evident within some trabeculae.

4.5 Fibula

Associated with the transversally sectioned tibia, a cross section of an undetermined long bone was also studied. Based on its size, shape and degree of association with the tibia, we interpret this element as a fibula. The section reveals the presence of a thin cortex of compact bone that surrounds a free medullary cavity. As in the other long bones, no ICL is present. The cortical bone is composed of uninterrupted woven-fibred bone tissue with primary osteons in early stages of development. The pattern of vascularisation varies in the different portions of the compacta: in some areas it is laminar, while in other areas radial canals predominate. No particular differences were observed as compared to other long bones studied.

4.6 Astragalus

A complete section was obtained for histological analysis. The microanatomy of this element largely differs from that of the previously described bones. The astragalus is composed of highly porous (fine cancellous) bone tissue and lacks a well-defined medullary cavity. Only a small peripheral region (which corresponds to the articular facet for the tibia) reveals the presence of a thin (0.35 mm) layer of compact bone tissue. Unfortunately, the poor preservation of the sample precludes a proper characterisation of the bone tissue. Although the internal vascular spaces are mostly irregular in shape and size, in some areas (particularly towards the ventral surface) there appears to be a radial arrangement of the canals from the centre of the element towards the periphery (Figure 4(C)). The outer region of the bone is coated by a thin layer of hypertrophied calcified cartilage (Figure 4(D)).

4.7 Dorsal ribs

The transverse sections of the ribs have a distinct outer cortex that surrounds a medullary region (Figure 4(E)). The perimedullary region of the cortex contains some resorption cavities. A thin layer of endosteally formed lamellar tissue is partially developed in the perimedullary cortex (Figure 4(F)). The cortical bone is entirely composed of woven-fibred bone tissue (Figure 4(G),(H)). Vascular spaces are surrounded by flattened osteocyte lacunae, indicating the early formation of primary osteons. The orientation of the vascular canals of the cortical bone varies in the cross section: the medial cortex contains abundant longitudinally oriented vascular spaces, whereas in the lateral cortex the canals exhibit a more variable arrangement (ranging from longitudinal to radial orientations) and they are less abundant. Also, the channels in the lateral cortex are larger ($\approx$0.06 mm diameter) than in the medial cortex ($\approx$0.03 mm). No growth marks were recorded.

4.8 Autopodial bones

The same block that contains the above described longitudinal section of a tibia and an astragalus also reveals the presence of three closely associated small bones. We refer to these elements as autopodial bones of the hindlimb, since more accurate identification of these bones is not possible. The plane of sectioning was also undeterminable, and we therefore only provide a general description of the histological features. Except for the largest element that is

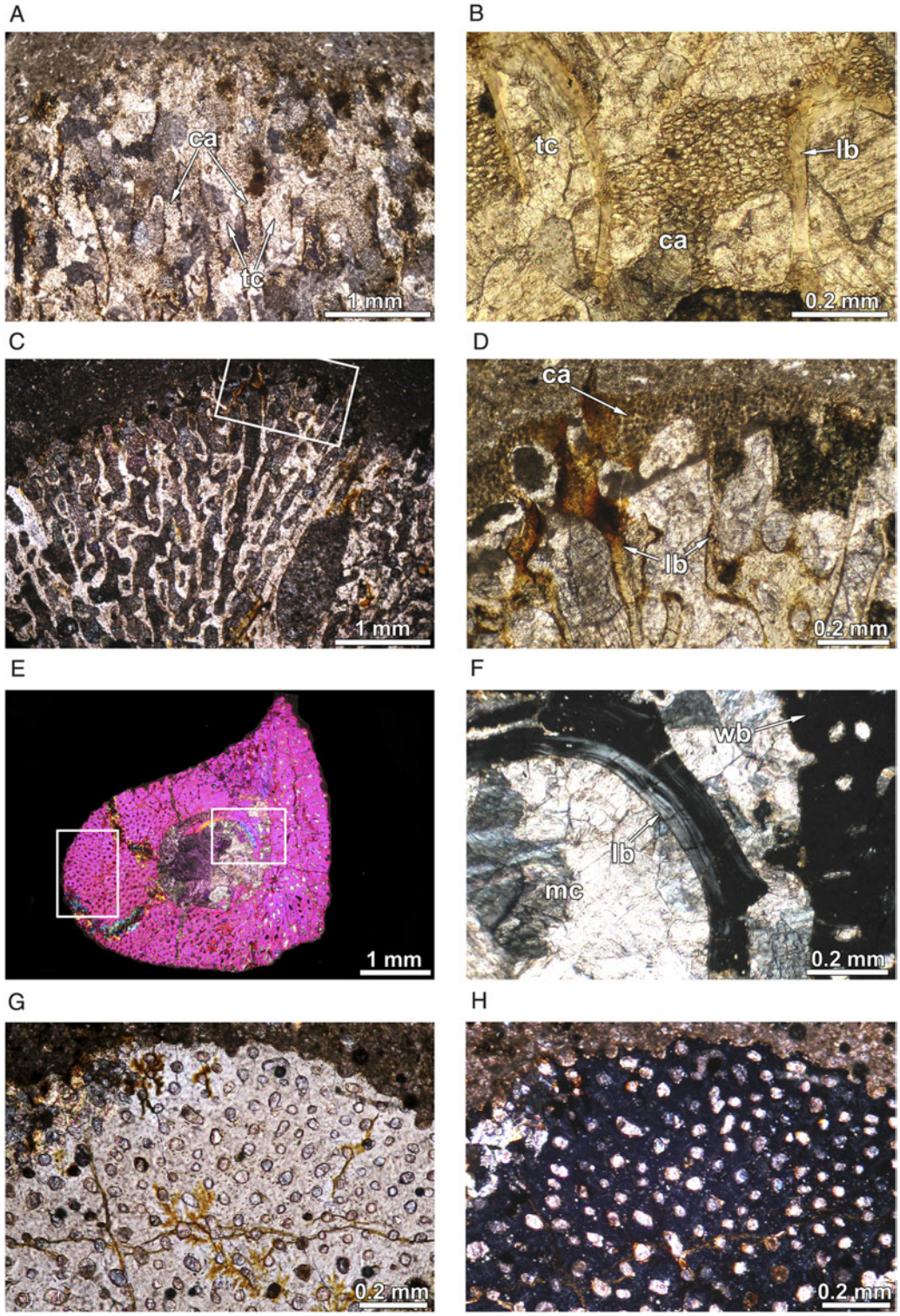

Figure 4. Bone microstructure of juvenile specimens of *M. patagonicus*. (A) Distal end of the tibia in longitudinal section. The section is composed of calcified cartilage with longitudinally oriented transphyseal canals. Polarised light. (B) Details of the 'epiphyseal' calcified cartilage. The transphyseal canals are coated by a thin layer of lamellar bone. Normal light. (C) Distal portion of the astragalus. Normal light. (D) Higher magnification of the same specimen (box inset in C). The outer region is coated by calcified cartilage. Normal light. (E) Dorsal rib in cross section. Polarised light with lambda compensator. (F) Details of the endosteal lamellar bone at the perimedullary cortex of the same specimen (smaller box inset in E). Polarised light. (G) Close up of the outer cortex of the same specimen (larger box inset in E). Vascular spaces are mainly longitudinally oriented. Note that the periosteal margins are uneven, with vascular spaces open to the sub-periosteal margin. Normal light. (H) The same section under polarised light. Abbreviations: ca, calcified cartilage; lb, lamellar bone tissue; mc, medullary cavity; tc, transphyseal canals; vc, vascular canals; wb, woven-fibred bone tissue.

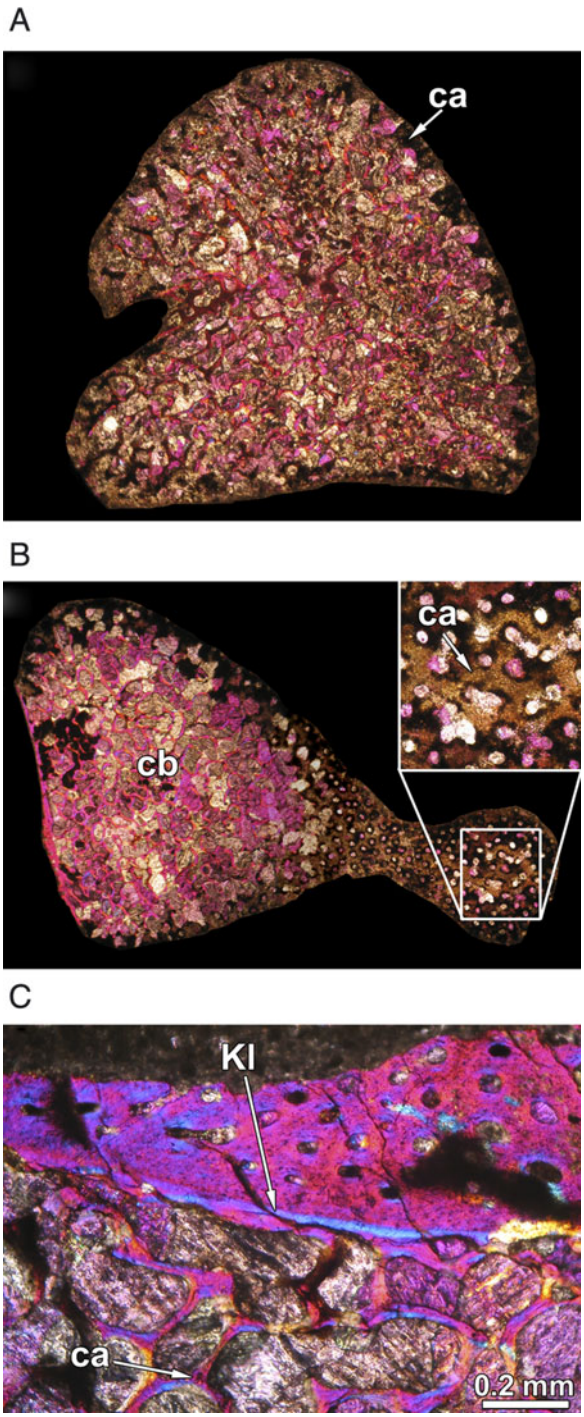

Figure 5. Bone microstructure of juvenile specimens of *M. patagonicus*. (A) Complete section of an undetermined autopodial bone. The bone is almost entirely composed of cancellous bone. Polarised light with lambda compensator. (B) Undetermined bone. The section is mostly composed of cancellous bone and calcified cartilage. Upper right corner in B: higher magnification of the calcified cartilage. Polarised light with lambda compensator. (C) Undetermined bone. The compact and cancellous bone tissues are separated by a Kastchenko's line. Remains of calcified cartilage are observable within some trabeculae. Polarised light with lambda compensator. Abbreviations: ca, calcified cartilage; cb, cancellous bone; Kl, Kastchenko's line.

formed by both compact and cancellous bone, the sectioned portions of the autopodial bones consist entirely of cancellous bone (Figure 5(A)). Bony trabeculae are composed of endosteal lamellar bone. The outer portions of the bones are coated by a thick layer of hyperthophied calcified cartilage or a layer of compact bone of variable thickness.

4.9 Undetermined bones

Several undetermined bones were observed in the sectioned blocks of specimen MPM-PV 1813/12. These elements (in which the position and section plane cannot be established) are commonly composed of a thin cortex surrounding a cancellous core or consist entirely of cancellous tissue (Figure 5(B),(C)). In some bones, a Kastchenko's line (Francillont-Vieillot et al. 1990; Ricqlès et al. 2001; Erismis and Chinsamy 2010), which marks the periphery of the initial cartilaginous *anlage*, prior to the onset of periosteal ossification, is observed at the boundary between the woven-fibred cortex and the cancellous bone tissue of the marrow cavity (Figure 5(E)). In these elements, calcified cartilage is visible within the bony trabeculae of the cancellous bone.

5. Discussion

5.1 Ontogenetic stage and growth dynamics

In accord with the small dimensions of the bones, the bone histology of the specimens examined revealed that they were at an early ontogenetic stage. The cortical bone tissue is entirely composed of a highly vascularised woven-fibred bone, in which the channels within the bone are large and unfilled, or in some cases just beginning to have thin deposits of lamellar bone. This kind of histological organisation has been reported in the earliest stages of fibrolamellar bone formation in dinosaurs and other fast growing vertebrates (e.g. Horner et al. 2000; Chinsamy-Turan 2005; Klein and Sander 2008; Hübner 2012). Other histological features that characterise the early ontogenetic stage of the individuals are lack of an ICL, absence of secondary osteons and growth marks, and presence of a thick layer of hypertrophied calcified cartilage in the epiphyseal regions of the long bones.

The absence of growth marks could be explained by remodelling during the expansion of the medullary cavity, although this appears to be rather unlikely. Growth marks were absent not only in the femora but also in several other postcranial bones, including dorsal ribs, which appear to be one of the best bones for skeletochronology (Erickson 2005; Pol et al. 2011; Waskow and Sander 2011). Most importantly, several adult sauropodomorph individuals collected at the Laguna Colorada locality and originally referred to as *Plateosaurus* by Casamiquela (1980) have recently been assigned to *M. patagonicus* by Otero and Pol (in press). This corroborated previous suggestions (Galton 1990; Galton and Upchurch 2004; Pol and Powell 2005; Salgado

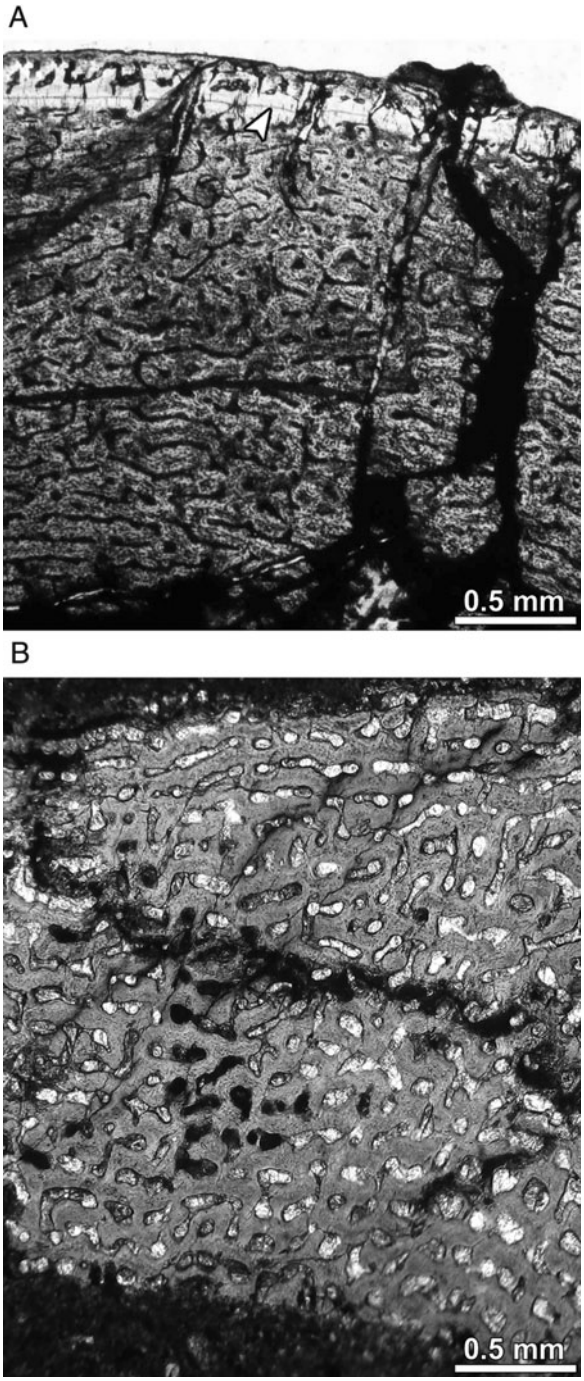

Figure 6. Comparative histology of the femora of *M. carinatus* BP/1/5253 (A) and *M. patagonicus* MPM-PV 1813/10 (B). The cortical bone of *Massospondylus* exhibits a distinct LAG (arrowhead) and is more compact than that observed in *Mussaurus*.

and Bonaparte 2007). The juveniles described here are much smaller than these adult specimens recently referred to as *Mussaurus* (the femur length of the largest adult specimen is 80 cm). Macroscopic observation of the cortical bone of broken surfaces of these adult specimens reveals the presence of growth cycles, suggesting that growth marks were formed during the later stages of development. Assuming that growth lines are annually formed (e.g. Chinsamy 1993), it is reasonable to assume that the specimens of *Mussaurus* studied here had not yet reached the first year of growth of growth when they demised. Given that the 14 specimens that are closely associated with the original block vary only slightly in terms of body size (femur length varies between 111 and 120 mm), we assume that they were all approximately the same age.

Another possible explanation for the absence of growth marks in *Mussaurus* could be related to a continuous (uninterrupted) growth during the first stages of development. Growth marks are absent or poorly developed in the long bones of sauropod dinosaurs during the early ontogenetic stages (Sander 2000; Sander et al. 2004, 2011a; Klein and Sander 2008). If *Mussaurus* had the same growth pattern as observed in sauropod dinosaurs, the juvenile specimens studied here could actually be more than a year old. However, as mentioned above, a previous histological study on basal sauropodomorph *M. carinatus* (Chinsamy 1993) indicate that, at least in this species, growth marks were recorded even in the smallest individual sampled (femur length 12.75 cm) (Figure 6). Based on the study of *Massospondylus* and that of *Plateosaurus* (Chinsamy 1993; Klein and Sander 2008), we consider the deposition of growth marks through the ontogeny as the most conservative hypothesis for the growth strategy for *Mussaurus*. Further histological analyses of *Mussaurus* individuals of different ontogenetic stages (particularly juveniles and sub-adults) are necessary to test this hypothesis.

5.2 Inferences on the early growth rate

Based on the assumption that the studied specimens died before reaching the first year of growth, we can use the bone histology of *Mussaurus* to obtain information on the early growth of this species. If we compare the body mass of the juvenile specimens studied here with the body mass of the neonate individuals (inferred from the size of the eggs), an estimation of the early growth rate can be deduced. Based on the dimensions of the largest egg assigned to *Mussaurus* (60 × 45 mm) (Bonaparte and Vince 1979), we estimated the egg volume (volume = 4/3 πab^2, where '*a*' and '*b*' are the largest and the minimal diameters of the eggs) and calculated the maximum neonate body mass using the density value proposed for dinosaurs (1000 kg per cubic metre; see Alexander 1989). We deduce that the maximum body mass of the neonate individuals of *Mussaurus* was approximately 0.063 kg. Considering the presence of a considerable amount of fluids and extraembryonic membranes within the eggs, the neonate body mass was probably less than the calculated maximum value. Using the regression equation based on femoral minimum shaft circumference proposed by Anderson et al. (1985) (later modified by Alexander 1989) for body mass estimation in quadrupedal vertebrates, we

estimated a body mass of 23 kg for MPM-PV 1813/10. This suggests that *Mussaurus* hatchlings would have gained more than 20 kg during their first year of life.

Our data on *Mussaurus* can be directly compared with that of *M. carinatus* (Chinsamy, 1993). In the sample of *Massospondylus* analysed by Chinsamy (1993), the smallest specimen studied (BP/1/5253) is approximately equal in size to the *Mussaurus* specimens studied here (femur length and minimal shaft circumference in *Massospondylus* BP/1/5253 equals to 127.5 and 51.23 mm, respectively). The main difference pertains to the relative porosity of the compact bone tissue in the femur. The femoral cortex of BP/1/5253 (Figure 6(A)) is clearly more compact (vascular spaces diameter 15–25 μm) than that observed in *Mussaurus* (vascular spaces diameter 25–80 μm) (Figure 4(B)). A higher porous cortical bone is typically indicative of a higher rate of bone deposition, which occurs commonly during the earlier stages of development (Horner et al. 2001; Chinsamy-Turan 2005). The sampled bones of *Mussaurus* lacks any growth marks, but in the femur of BP/1/5253 a single LAG was visible in the cortex (Figure 4(A)). Moreover, Chinsamy (1993) proposed that it is possible that an earlier LAG may have been obliterated due to medullary expansion. Interestingly enough the *Mussaurus* and *Massospondylus* bones are from similar-sized femora, the bone microstructure of *Mussaurus* is clearly from an earlier ontogenetic stage.

Comparing the age and body mass of the juveniles specimens of *Mussaurus* and *Massospondylus* provides some clues about the early growth rate in both taxa. The estimated body mass for BP/1/5253 (21 kg) is comparable with the 23 kg obtained for a similar-sized *Mussaurus* specimen. As previously mentioned, a well-developed LAG was recorded near the peripheral region of the cortex of the femur of specimen BP/1/5253 (Figure 6(A)). Based on the zone thickness observed in thin sections of several specimens of *Massospondylus*, Chinsamy (1993) estimated an ontogenetic age of 2 years for the specimen BP/1/5253. Hence, while an individual of *Mussaurus* would have reached a body mass of 23 kg in less than a year, *Massospondylus* would have needed about 2 years to reach an almost equivalent body mass. Assuming that the egg size correlates with neonate body size, and given that the eggs of *Mussaurus* and *Massospondylus* have the same diameters (60 mm [Reisz et al. 2005]), we considered that the body mass in the neonate individuals of both taxa was similar. Therefore, although both taxa start their growth with similar body sizes, *Mussaurus* seems to have had a faster early growth rate than *Massospondylus*.

6. Concluding remarks

Although the juvenile specimens of *M. patagonicus* described here are markedly larger than the post-hatchling specimens described by Bonaparte and Vince (1979) (i.e. femur of the juveniles is four times larger in length than those of the post-hatchlings), the bone histology of the juvenile specimens reveals that they still were at an early ontogenetic stage. The bone microstructure of these specimens also indicates a rapid rate of growth during early ontogeny in *M. patagonicus*, which appears to be faster than that of the basal sauropodomorph *M. carinatus*. Given the large adult body size of *M. patagonicus* and that this species has been interpreted as being more closely related to sauropods than both *Plateosaurus* and *Massospondylus* (2004; Pol and Powell 2007; Sereno 2007; Otero and Pol in press), the study of the bone microstructure of this taxon is particularly important to understand the evolution of gigantism in Sauropodomorpha and the evolutionary origins of the sauropod-type growth strategy (Sander et al. 2004, 2011a). Previous studies on sauropod bone histology (Sander 2000; Sander et al. 2004, 2011a; Klein and Sander 2008) described the 'typical' sauropod long-bone microstructure as consisting of a cortex of the well-vascularised laminar fibrolamellar bone devoid of growth marks (except in the cortical periphery). This type of bone tissue has been interpreted as indicative of sustained, accelerated skeletal growth which may have made the gigantism of such dinosaurs possible (Sander et al. 2004, 2011b). On the other hand, the long bone histology basal sauropodomorphs as *Plateosaurus* and *Massospondylus* consist of primary bone of the laminar fibrolamellar type interrupted by LAGs and has been interpreted as a slower growth rate (Sander et al. 2004). Future studies of additional material of *M. patagonicus* will be important to evaluate whether the growth in later ontogenetic stages of *Mussaurus* was cyclic as reported for other basal sauropodomorphs or they had a sauropod-like growth strategy. The higher early growth rate inferred in *Mussaurus* could be related to the origin of the rapid growth rates observed in more derived sauropodomorph dinosaurs, which allowed the evolution of gigantism in this lineage.

Acknowledgements

We would like to thank the Subecretaría de Cultura of Santa Cruz Province and the Museo Provincial Padre M.J. Molina for their collaboration and support on the field project conducted in El Tranquilo Group. We are thankful to P. Puerta, M. Cardenas, S. Reuil, D. Pais, A. Scanferla, A. Mancuso, M. Puerta and A. Lecuona for their participation in the field season. Part of this project was developed with the financial support of the Division of Paleontology (AMNH) and NSF grants DEB 0946430, DEB 1068089 (GWR); National Geographic Society Research Grant 8860-10 (to D.P.); Ministerio de Ciencia, Tecnología e Innovación Productiva of the República Argentina and Department of Science and Technology of South African Republic (SA/11/15 to D.P. and A.C.) and Agencia Nacional de Promoción Científica y Tecnológica (PICT-2011-1181 to I.A.C.). Preparation of the specimens MPM was executed by P. Puerta, M. Caffa, L. Canesa and J.L. Carballido. Histological sections were prepared by M. Caffa. J.L. Carballido, J. M. Leardi and A. Otero, providing measurements of different specimens of *Mussaurus* and *Massospondylus*. A. Otero and an anonymous reviewer improved the manuscript with constructive comments.

References

Alexander RMcN. 1989. Dynamics of dinosaurs and other extinct giants. New York: Columbia University Press.

Anderson JF, Hall-Martin A, Russell DA. 1985. Long-bone circumference and weight in mammals, birds and dinosaurs. J Zool (Lond). 207:53–61.

Bonaparte JF, Vince M. 1979. El hallazgo del primer nido de Dinosaurios Triásicos (Saurischia, Prosauropoda), Triásico Superior de Patagonia, Argentina. Ameghiniana. 16:173–182.

Casamiquela RM. 1980. La presencia del género *Plateosaurus* (Prosauropoda) en el Triásico Superior de la Formación El Tranquilo, Patagonia. Actas II Congr Arg Paleontol Bioestrat I Congr Latinoam Paleontol. 1:143–158.

Cerda IA, Chinsamy A. 2012. Biological implications of the bone microstructure of the Late Cretaceous ornithopod dinosaur *Gasparinisaura cincosaltensis*. J Vert Paleontol. 32:355–368.

Chinsamy A. 1990. Physiological implications of the bone histology of *Syntarsus rhodesiensis* (Saurischia; Theropoda). Paleontol Afr. 27:77–82.

Chinsamy A. 1993. Bone histology and growth trajectory of the prosauropod dinosaur *Massospondylus carinatus* (Owen). Mod Geol. 18:319–329.

Chimsamy A, Raath MA. 1992. Preparation of fossil bone for histological examination. Paleontol Afr. 29:39–44.

Chinsamy-Turan A. 2005. The microstructure of dinosaur bone. Baltimore: Johns Hopkins University Press.

Company J. 2011. Bone histology of the titanosaur *Lirainosaurus astibiae* (Dinosauria: Sauropoda) from the Latest Cretaceous of Spain. Naturwissenschaften. 98:67–78.

Curry KA. 1999. Ontogenetic histology of *Apatosaurus* (Dinosauria: Sauropoda): new insights on growth rates and longevity. J Vert Paleontol. 19:654–665.

Erickson GM. 2005. Assessing dinosaur growth patterns: a microscopic revolution. Trends Ecol Evolut. 20:677–684.

Erickson GM, Curry-Roger K, Yerby SA. 2001. Dinosaurian growth patterns and avian rapid growth rates. Nature. 412:429–433.

Erickson GM, Curry-Rogers K, Varrichio DJ, Norell MA, Xu X. 2007. Growth patterns in brooding dinosaurs reveals the timing of sexual maturity in non-avian dinosaurs and genesis of the avian condition. Biol Lett. 3:558–561.

Erismis UC, Chinsamy A. 2010. Ontogenetic changes in the epiphyseal cartilage of *Rana* (*Pelophylax*) *caralitana* (Anura: Ranidae). Anat Rec. 293:1825–1837.

Francillon-Vieillot H, de Buffrénil V, Castanet J, Géraudie J, Meunier FJ, Sire JY, Zylberberg L, Ricqlès AJde. 1990. Skeletal biomineralization: Patterns, Processes and Evolutionary Trends. In: Carter JG, editor. Microstructure and mineralization of vertebrate skeletal tissues. Vol. 1. New York: Van Nostrand Reinhold. p. 471–548.

Galton PM. 1990. The Dinosauria. In: Weishampel DB, Dodson P, Osmólska H, editors. Basal Sauropodomorpha. Berkeley: University of California Press. p. 320–344.

Galton PM, Upchurch P. 2004. The Dinosauria. 2nd ed. p. 232–258.

Haines RW. 1942. The evolution of epiphyses and of endochondral bone. Biol Rev. 174:267–292.

Hayashi S, Carpenter K, Suzuki D. 2009. Different growth patter between the skeleton and osteoderms of *Stegosaurus* (Ornithischia: Thyreophora). J Vert Paleontol. 29:123–131.

Herbst R. 1965. La flora fósil de la Formación Roca Blanca, provincia Santa Cruz, Patagonia, con consideraciones geológicas y estratigráficas. Opera Lilloana. 12:1–101.

Horner JR, Ricqlès AJde, Padian K. 2000. The bone histology of the hadrosaurid dinosaur Maiasaura peeblesorum: growth dynamics and physiology based on an ontogenetic series of skeletal elements. J Vert Paleontol. 20:109–123.

Horner JR, Padian K, Ricqlès AJde. 2001. Comparative ostehistology of some embryonic and perinatal archosaurs: developmental and behavioral implications for dinosaurs. Paleobiology. 27:39–58.

Horner JR, Ricqlès AJde, Padian K, Scheetz RD. 2009. Comparative long bone histology and growth of the 'hypsilophodontid' dinosaurs *Orodromeus makelai, Dryosaurus altus*, and *Tenontosaurus tilletii* (Ornithischia: Euornithopoda). J Vert Paleontol. 29:734–747.

Hübner TR. 2012. Bone histology in *Dysalotosaurus lettowvorbecki* (Ornithischia: Iguanodontia) – variation, growth, and implications. PLoS ONE. 7(1):e29958.

Jalfin GA, Herbst R. 1995. La flora triásica del grupo El Tranquilo, Provincia de Santa Cruz (Patagonia). Estratigrafía. Ameghiniana. 32:211–229.

Klein N, Sander PM. 2007. Bone histology and growth of the prosauropod dinosaur *Plateosaurus engelhardti* Von Meyer, 1837 from the Norian bonebeds of Trossingen (Germany) and Frick (Switzerland). Spec Pap Palaeontol. 77:169–206.

Klein N, Sander PM. 2008. Ontogenetic stages in the long bone histology of sauropod dinosaurs. Paleobiology. 34:247–263.

Klein N, Sander PM, Stein K, Le Loeuff J, Carballido JL, Buffetaut E. 2012. Modified laminar bone in *Ampelosaurus atacis* and other titanosaurs (Sauropoda): implications for life history and physiology. PLoS ONE. 7(5):e36907.

Lee AH, Werning S. 2008. Sexual maturity in growing dinosaurs does not fit reptilian growth models. Proc Natl Acad Sci USA. 105:582–587.

Lehman TM, Woodward HN. 2008. Modeling growth rates for sauropod dinosaurs. Paleobiology. 24:264–281.

Otero A, Pol D. in press. Postcranial anatomy and phylogenetic relationships of *Mussaurus patagonicus* (Dinosauria, Sauropodomorpha). J Vert Paleontol.

Padian K, Horner JR, Ricqlès AJde. 2004. Growth in a small dinosaur and pterosaurs: the evolution of archosaurian growth strategies. J Vert Paleontol. 24:555–571.

Pol D, Garrido A, Cerda IA. 2011. A new sauropodomorph dinosaur from the Early Jurassic of Patagonia and the origin and evolution of the sauropod type sacrum. PLoS ONE. 6(1):e14572.

Pol D, Powell JE. 2005. Anatomy and phylogenetic relationships of *Mussaurus patagonicus* (Dinosauria, Sauropodomorpha) from the Late Triassic of Patagonia. Bol Resum/II Cong L-A Paleontol Vert. 2:208.

Pol D, Powell JE. 2007. Skull anatomy of *Mussaurus patagonicus* (Dinosauria: Sauropodomorpha) from the Late Triassic of Patagonia. Hist Biol. 19:125–144.

Reid REH. 1997. The Complete Dinosaur. In: Farlow JO, Brett-Surman MK, editors. How dinosaur grew. Bloomington & Indianopolis: Indiana University Press. p. 307–316.

Reisz RR, Scott DM, Sues H-D, Evans DC, Raath MA. 2005. Embryos of an Early Jurassic prosauropod dinosaur and their evolutionary significance. Science. 309:761–764.

Ricqlès AJde. 1980. A cold look at the warm-blooded dinosaurs. In: Thomas RDK, Olson EC, editors. Tissue structure of the dinosaur bone: functional significance and possible relation to dinosaur physiology. Boulder: Westview press. p. 103–139.

Ricqlès A de, Mateus O, Antunes MT, Taquet P. 2001. Histomorphogenesis of embryos of Upper Jurassic theropods from Lourinhã (Portugal). C R Acad Sci Paris 332:647–656.

Rimblot-Baly F, Ricqlès AJ, de Zylberberg L. 1995. Analyse paléohistologique d'une série de croissance partielle chez *Lapparentosaurus madagascariensis* (Jurassique moyen): essay sur la dynanique de croissance d'un dinosaure sauropode. Ann Paléontol. 81:49–86.

Salgado L, Bonaparte JF. 2007. Patagonian Mesozoic Reptiles. In: Gasparini Z, Salgado L, Coria RA, editors. Sauropodomorpha. Indiana: Indiana University Press. p. 188–228.

Sander PM. 2000. Long bone histology of the Tendaguru sauropods: implications for growth and biology. Paleobiology. 26:466–488.

Sander PM, Christian A, Clauss M, Fechner R, Gee CT, Griebeler EM, Gunga HC, Hummel J, Mallison H, Perry SF, et al., 2011b. Biology of the sauropod dinosaurs: the evolution of gigantism. Biol Rev Camb Philos Soc. 86:117–155.

Sander PM, Klein N. 2005. Unexpected developmental plasticity in the life history of an early dinosaur. Science. 310:1800–1802.

Sander PM, Klein N, Buffetaut E, Cuny G, Suteethorn V, Loeuff JL. 2004. Adaptative radiation in sauropod dinosaurs: bone histology indicates rapid body size acceleration. Org Divers Evol. 4:165–173.

Sander PM, Klein N, Stein K, Wings O. 2011a. Biology of the Sauropods Dinosaurs. In: Klein N, Remes K, Gee CT, Sander PM, editors. Sauropod bone histology and its implications for sauropod biology. Bloomington and Indianapolis: Indiana University Press. p. 274–300.

Sander PM, Mateus O, Laven T, Knötschke N. 2006. Bone histology indicates insular dwarfism in a new Late Jurassic saurópodo dinosaur. Nature. 441:739–741.

Sander PM, Tückmantel C. 2003. Bone lamina thickness, bone apposition rates, and age estimates in sauropod humeri and femora. Paläontol Zeit. 77:161–172.

Starck JM, Chinsamy A. 2002. Bone microstructure and developmental plasticity in birds and others dinosaurs. J Morph. 245:232–246.

Stein K, Csiki Z, Curry-Rogers K, Weishampel DB, Redelstorff R, Carballido JL, Sander PM. 2010. Small body size and extreme cortical bone remodeling indicate dwarfism in *Magyarosaurus dacus* (Sauropoda: Titanosauria). Proc Natl Acad Sci USA. 107:9258–9263.

Varricchio DJ. 1993. Bone microstructure of the Upper Cretaceous theropod dinosaur *Troodon formosus*. J Vert Paleontol. 13:99–104.

Varricchio DJ. 1997. Encyclopedia of Dinosaurs. In: Currie PJ, Padian K, editors. Growth and embryology. San Diego: Academic Press. p. 282–288.

Waskow K, Sander PM. 2011. The age of giants; histological evidence for ontogeny in postcranial elements of sauropods and its implications for growth history. Soc Vert Paleontol, Ann Meet Abst. 31:212A.

Werning S. 2012. The ontogenetic osteohistology of *Tenontosaurus tilletti*. PLoS ONE. 7(3):e33539.

Woodward HN, Lehman TM. 2009. Bone histology and microanatomy of *Alamosaurus sanjuanensis* (Sauropoda: Titanosauria) from the Maastrichtian of Big Bend National Park, Texas. J Vert Paleontol. 29:807–821.